Formal Analysis Provides Parameters for Guiding Hyperoxidation in Bacteria using Phototoxic Proteins

Qinsi Wang
Computer Science Department
Carnegie Mellon University
qinsiw@cs.cmu.edu

Natasa Miskov-Zivanov
Electrical and Computer Engineering Department
Carnegie Mellon University
nmiskov@andrew.cmu.edu

Cheryl Telmer
Biological Sciences Department
Carnegie Mellon University
ctelmer@cmu.edu

Edmund M. Clarke
Computer Science Department
Carnegie Mellon University
emc@cs.cmu.edu

ABSTRACT

In this work, we developed a methodology to analyze a bacteria model that mimics the stages through which bacteria change when phage therapy is applied. Due to the widespread misuse and overuse of antibiotics, drug resistant bacteria now pose significant risks to health, agriculture and the environment. Therefore, we were interested in an alternative to conventional antibiotics, a phage therapy. Our model was designed according to an experimental procedure to engineer a temperate phage, Lambda (λ), and then kill bacteria via light-activated production of superoxide. We applied formal analysis to our model and the results show that such an approach can speed up evaluation of the system, which would be impractical or possibly not even feasible to study in a wet lab.

1. INTRODUCTION

The discovery of antibiotics has been quickly followed by the development of antibiotic resistance. New medicines are becoming increasingly scarce in tackling this issue. The document released by CDC (Centers for Disease Control and Prevention), "Antibiotic Resistance Threats in the United States, 2013" [1], intends to raise public awareness of the problems associated with overuse and misuse of antibiotics and to outline the threats to society caused by these organisms. The organisms have been categorized by hazard level as urgent, serious and concerning. Over 2 million illnesses and $23,000$ deaths per year are a direct result of antibiotic resistance.

There are multiple mechanisms of antibiotic resistance. First, altered permeability of the antimicrobial agent is suggested to be due to the inability of the agent to enter the bacterial cell, or alternatively, due to the active export of the agent from the cell. Second, resistance is often the result of the production of an enzyme that is capable of inactivating the antimicrobial agent. Next, resistance can arise due to alteration of the target site for the antimicrobial agent. Finally, resistance can result from the acquisition of a new enzyme to replace the sensitive one, thus replacing the pathway that was originally sensitive to antibiotic to another pathway.

The CDC outlines four core actions that will help fight deadly infections [1]: (a) preventing infections and the spread of resistance; (b) tracking resistant bacteria; (c) improving the use of today's antibiotics; and (d) promoting the development of new antibiotics and developing new diagnostic tests for resistant bacteria. Recently, we have addressed this problem by designing a new system that relies on phage-based therapy. Phages, or bacteriophages, are viruses that infect bacteria and have evolved to manipulate the bacterial cells and genome, making resistance to bacteriophages difficult to achieve. Bacteriophages are complex and utilize many host pathways such that they cannot be inactivated or bypassed. Bacteriophages infect only specific hosts and can kill the host by cytolysis. However, many phages are temperate, meaning that they can enter a lysogenic phase and therefore not lyse and kill the host bacteria. The addition of a phototoxic protein to the system offers a second method of killing those bacteria targeted by a lysogenic phage. Thus, our system, shown in Figure 1, explores the possibility that temperate phages can also be used for phage therapy and bacteria killing applications. We incorporated several proteins (KillerRed [8], SuperNova [10]), that have been shown to be phototoxic and that provide another level of controlled bacteria killing.

In this paper, we describe our computational model of the phage-bacteria system in section 2, which has been developed as an extension of an initial model described in [2]. Then, a formal analysis technique used to deal with the parameter estimation and parameter sensitivity evaluation of our hybrid model is introduced in section 3. Section 4 presents the analysis results, and demonstrates that our model and methodology allow for studying the behavior and final state of the system at a number of points in the pa-

GLSVLSI'15, May 20–22, 2015, Pittsburgh, PA, USA.

http://dx.doi.org/10.1145/2742060.2743762.

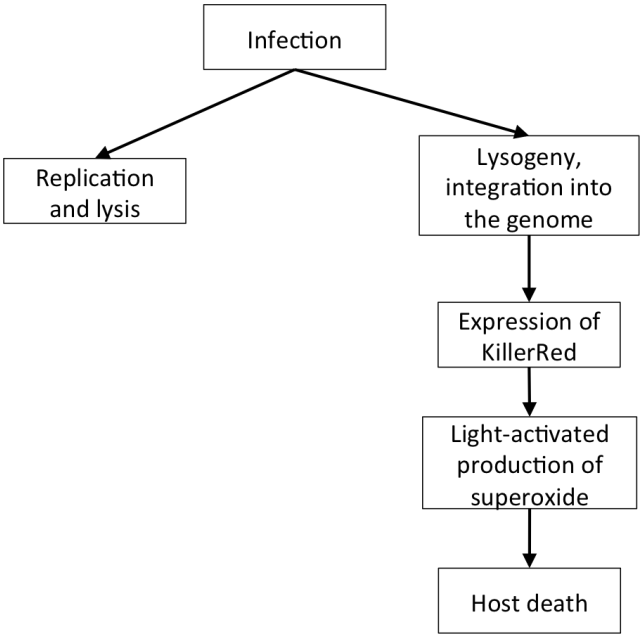

Figure 1: Interactions between phage and bacteria used in our model

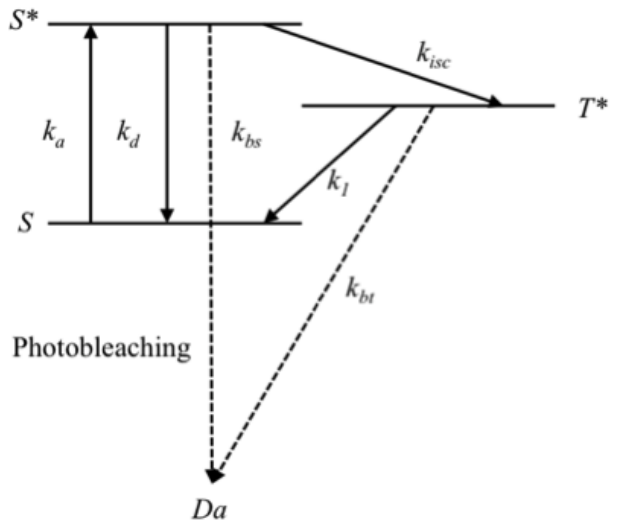

Figure 2: Energy diagram for a generic fluorochrome [9]

rameter space, and for checking properties that are often impractical to characterize using wet lab procedures only. Section 5 concludes the paper.

2. THE KILLERRED MODEL

We have modeled synthesis and action of KillerRed that occurs over three main phases of a typical photobleaching experiment: induction at 37°C, storage at 4°C to allow for protein maturation, and photobleaching at room temperature. Within these phases, we identify several stages of interest in KillerRed synthesis and activity as follows.
- mRNA synthesis and degradation
- KillerRed synthesis, maturation, and degradation
- KillerRed states: singlet (S), singlet excited (S^*), triplet excited (T^*), and deactivated (Da)
- Superoxide production (by KillerRed)
- Superoxide elimination (by superoxide dismutase)

We implemented these system stages with distinct model states, and outlined them in Figure 3, together with state variables (values are included if variables are fixed within a state), transitions between states, and events that trigger state transitions. In Table 1 we list the model states that are used to describe the stages of the system. In the following, we detail our implementation of system stages within the model. We also list equations that we derived for each stage.

Cell exposure to light
In [11], the authors describe a method for determining the rate coefficient of activation from the ground state k_a: $k_a = \sigma I$. In detail, σ is the optical cross-section per molecule and I is the excitation intensity in photons per unit area. The lamp used for photobleaching gave $I = 11027\ photons/cm^2 s$ (about $1W$). σ is given by $\sigma = \varepsilon(1000cm^3/L)(ln10)NA$, where ε is the extinction coefficient and NA is Avogadro's number. We calculated $k_a = 1.721011 s^{-1}$ for KillerRed for our photobleaching experiments. The rate constant for returning to the ground state is $k_f = ln2/\tau$, where τ is the half-life for KillerRed in the excited state. τ for KillerRed is assumed to be similar to τ for dsRed (about $3.0ns$ [3]), since their chromophores are identical. Thus, by assuming that KillerRed is always in the excited state (if it has not been deactivated) during photobleaching, we have that $k_f = 2.3108 s^1$ and $F = k_a/(k_a + k_f) = 0.9987$.

Production of superoxide
Production of the superoxide radical is governed by several reactions. Fluorescein is used as a model chromophore. S, S, T, and Da are the singlet, excited singlet, excited triplet, and deactivated states, respectively, of the chromophore. Figure 2 outlines transitions between different forms of the chromophore. In detail, fluorochrome molecules absorb photon energy at a rate k_a and go from the ground singlet state S up to the excited singlet state S^*. Then they may return to the ground state by radiative (fluorescence) or non-radiative (internal conversion) pathway at a combined rate k_d. They may also undergo non-radiative intersystem crossing, at a rate k_{isc}, to T^*, where they may return to the ground state at a rate k_1. Photobleaching may take place from both S^* and T^* at rates k_{bs} and k_{bt}, respectively. Those photobleached molecules can no longer participate in the excitation-emission cycle.

Superoxide dismutase
Superoxide dismutase is $E.\ coli's$ main defense against superoxide. Its action was incorporated using Michaelis-Menten kinetics:
$-\frac{d[O_2^{\cdot -}]}{dt} = \frac{V_{max}[O_2^{\cdot -}]}{K_m + [O_2^{\cdot -}]}$,
where V_{max} estimated using k_cat from [7], and K_m was estimated using k_m and k_{cat}/k_m from [4, 7].

Cell without λ-phage genome
The first system stage that we model is a bacteria cell that does not have phage genome injected, and gene transcription is not induced. Thus, all of the model elements are at their initial level, assumed to be 0. In the model, we assume that λ-phage genome is injected into bacteria cell with rate k_1, or t_1 time units after the start of time counting. When analyzing individual cells this does not have an effect, but

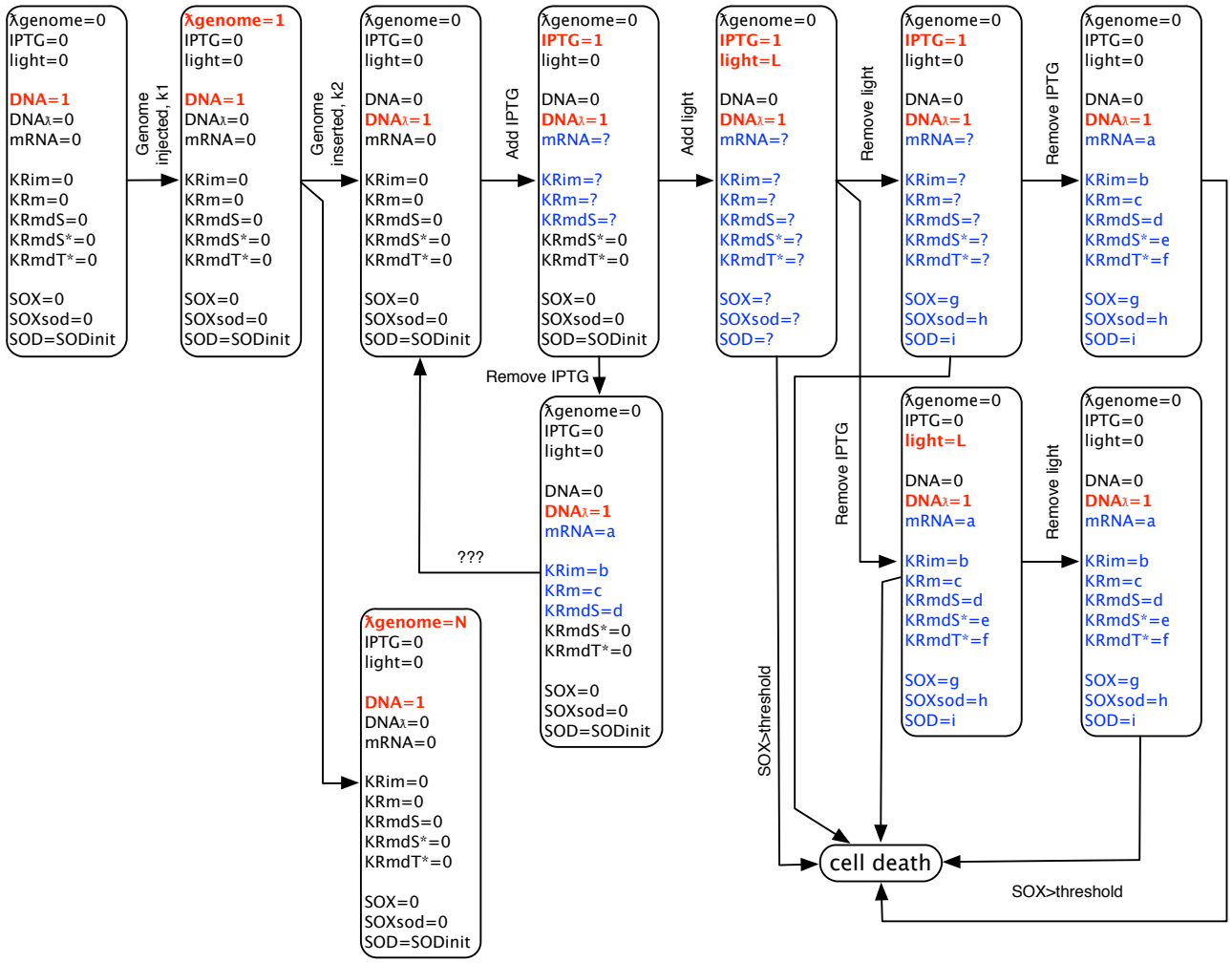

Figure 3: Hybrid automaton for our KillerRed model

is important to take into account when analyzing cell population.

Cell with injected λ-phage genome
After the injection of phage genome into the cell, the genome will be inserted into the bacterial DNA with rate k_2. Or, in terms of counting time units, it will take t_2 time units to integrate the phage genome into bacterial plasmid once it is inside the cell. However, since IPTG is still not added to the cell, we assume that gene transcription is not induced yet. Therefore, similar to previous two states, initial state and the state of phage genome injected, this state is assumed to be static.

Addition of IPTG
When IPTG is added to the system, the transcription starts. Measure of transcriptional efficiency is the rate of mRNA synthesis, k_{RNAsyn}. Our construct uses a wild-type lac promoter, so we assume that its transcription rates are similar to the lac operon. Next, mRNA transforms into immature KillerRed molecules with translational efficiency, k_{KRsyn}. The maximum translation rate in the model is three orders of magnitude lower to reflect the presents of several rare codons. This adjustment is suggested by comparisons of our fluorescence data for KillerRed and mRFP, which have nearly identical brightness.

Immature synthesized KillerRed (KR_{im}) requires additional time to become mature KillerRed form (KR_m), and to fold and create a dimer (KR_{md}). These two events together occur with the overall rate of k_{KR_m}. This folded and dimerized form of KillerRed that can be activated by light is called singlet form (KR_{mdS}). Degradations of synthesized mRNA and KillerRed in both modeled forms are included in equations with rates $k_{mRNAdeg}$ (characteristic half-life), $k_{KR_{im}deg}$, and k_{mdSdeg}, respectively. In this model state, resulting from addition of IPTG and ending with either removal of IPTG or addition of light, we use the following ordinary differential equations (ODEs) to describe the continuous dynamics.

$$\begin{aligned}
\frac{\mathrm{d}[mRNA]}{\mathrm{d}t} &= k_{RNAsyn} \cdot [DNA] - k_{RNAdeg} \cdot [mRNA] \\
\frac{\mathrm{d}[KR_{im}]}{\mathrm{d}t} &= k_{KR_{im}syn} \cdot [mRNA] - (k_{KR_m} + k_{KR_{im}deg}) \\
&\quad \cdot [KR_{im}] \\
\frac{\mathrm{d}[KR_{mdS}]}{\mathrm{d}t} &= k_{KR_m} \cdot [KR_{im}] - k_{KR_{mdS}deg} \cdot [KR_{mdS}]
\end{aligned}$$

State	State description	Input	Next state(s)
S_0	Initial system state, bacteria cell, without phage	n/a	S_1 (ex.)
S_1	Phage genome injected	λ-phage genome	S_2 (in.), S_3 (in.)
S_2	Phage genome replication (lytic cycle)	Genome replication	n/a
S_3	Phage genome within bacterial DNA (lysogenic cycle)	Genome insertion	S_4 (ex.)
S_4	Gene transcription, translation	Addition of IPTG	S_5 (ex.), S_6 (ex.)
S_5	Gene transcription decrease	Removal of IPTG	S_3 (in.) [1]
S_6	Activation of KillerRed	Light turned ON	S_7 (ex.), S_8 (ex.), S_{11} (in.)
S_7	Mixture of KillerRed forms, no activation	Light turned OFF	S_9 (ex.), S_{11} (in.)
S_8	Mixture of KillerRed forms, transcription decrease	Removal of IPTG	S_{10} (ex.), S_{11} (in.)
S_9	Mixture of KillerRed forms, no activation, transcription decrease	Removal of IPTG	S_{11} (in.)
S_{10}	Mixture of KillerRed forms, transcription decrease, no activation	Light turned OFF	S_{11} (in.)
S_{11}	Cell death	SOX>threshold	n/a

Table 1: List of modeled system states, their description, inputs and next state(s) with indication whether transition was triggered by external input (ex.) or by internal variable (in.) reaching some specified value.

Addition of light

Addition of light results in moving from the state with KillerRed synthesis into the state of activating KillerRed, S. In the state that assumes system's exposure to light, other forms of KillerRed are present, including excited singlet state S^*, (KR_{mdS^*}) and triplet state T^*, (KR_{mdT^*}). Transitions between different forms of KillerRed can occur and therefore, in this state, we include the above model equations and modified equation, and add equations for other forms of KillerRed (KR_{mdS^*}, KR_{mdT^*}), as well as equations for produced superoxide (SOX) and for the effect of superoxide dismutase (SOX_{sod}).

$$\begin{aligned}
\frac{\mathrm{d}[KR_{mdS}]}{\mathrm{d}t} &= k_{KR_m}\cdot[KR_{im}] + k_{KR_f}\cdot[KR_{mdS^*}] \\
&\quad + k_{KR_{ic}}\cdot[KR_{mdS^*}] + k_{KR_{nrd}}\cdot[KR_{mdT^*}] \\
&\quad + k_{KR_{SOXd1}}\cdot[KR_{mdT^*}] - k_{KR_{ex}}\cdot[KR_{mdS}] \\
&\quad - k_{KR_{mdS}deg}\cdot[KR_{mdS}] \\
\frac{\mathrm{d}[KR_{mdS^*}]}{\mathrm{d}t} &= k_{KR_{ex}}\cdot[KR_{mdS}] - k_{KR_f}\cdot[KR_{mdS^*}] \\
&\quad - k_{KR_{ic}}\cdot[KR_{mdS^*}] - k_{KR_{isc}}\cdot[KR_{mdS^*}] \\
&\quad - k_{KR_{mdS^*}deg}\cdot[KR_{mdS^*}] \\
\frac{\mathrm{d}[KR_{mdT^*}]}{\mathrm{d}t} &= k_{KR_{isc}}\cdot[KR_{mdS^*}] - k_{KR_{nrd}}\cdot[KR_{mdT^*}] \\
&\quad - k_{KR_{SOXd1}}\cdot[KR_{mdT^*}] \\
&\quad - k_{KR_{SOXd2}}\cdot[KR_{mdT^*}] \\
&\quad - k_{KR_{mdT^*}deg}\cdot[KR_{mdT^*}] \\
\frac{\mathrm{d}[SOX]}{\mathrm{d}t} &= k_{KR_{SOXd1}}\cdot[KR_{mdT^*}] + k_{KR_{SOXd2}} \\
&\quad \cdot[KR_{mdT^*}] - \frac{\mathrm{d}[SOX_{sod}]}{\mathrm{d}t} \\
\frac{\mathrm{d}[SOX_{sod}]}{\mathrm{d}t} &= k_{SOD}\cdot V_{maxSOD}\cdot\frac{[SOX]}{K_m+[SOX]}
\end{aligned}$$

Rates of KillerRed transitioning from state S^* to state S, through fluorescence or internal conversion are denoted with k_{KR_f} and $k_{KR_{ic}}$, respectively. Rates of KillerRed transitioning from state T^* to state S, through non-radiative deactivation or by production of SOX with deactivation are denoted with $k_{KR_{nrd}}$ and $k_{KR_{SOXd_1}}$, respectively. The excited form of KillerRed, S^*, is formed at rate $k_{KR_{ex}}$, and is reduced in several ways: (a) by fluorescence with rate k_{KR_f}, (b) by internal conversion with rate $k_{KR_{ic}}$, (c) by intersystem crossing $k_{KR_{isc}}$, and (d) by degradation with rate $k_{KR_{mdS^*deg}}$. The triplet form, T^*, is formed through intersystem crossing with rate $k_{KR_{isc}}$, and is reduced in several ways, by non-radiative deactivation with rate $k_{KR_{nrd}}$, by superoxide (ROS) production with deactivation to state S with rate $k_{KR_{SOXd_1}}$, by superoxide (ROS) production with photobleaching with rate $k_{KR_{SOXd_2}}$, and by degradation with rate $k_{KR_{mdS^*deg}}$. In addition, $k_{KR_{SOXd_1}}$ and $k_{KR_{SOXd_2}}$ can be computed taking into account relative propensity for KillerRed to generate superoxide without becoming deactivated (c), photo-bleaching rate obtained from experiments ($k_{KR_{pb}}$), and quantum yield (Φ) as follows.

$$k_{KR_{SOXd_1}} = c\cdot\frac{k_{KR_{pb}}}{\Phi} \qquad k_{KR_{SOXd_2}} = \frac{k_{KR_{pb}}}{\Phi}$$

3. δ-DECISIONS FOR HYBRID MODELS

In order to overcome the undecidability of reasoning about hybrid systems, Gao *et al.* recently defined the concept of δ-satisfiability over the reals, and presented a corresponding δ-complete decision procedure [5, 6]. The main idea is to decide correctly whether slightly *relaxed* sentences over the reals are satisfiable or not. The following definitions are from [6].

Definition 1 A bounded quantifier is one of the following:

$$\exists^{[a,b]}x = \exists x : (a \le x \wedge x \le b)$$
$$\forall^{[a,b]}x = \forall x : (a \le x \wedge x \le b)$$

Definition 2 A bounded Σ_1 sentence is an expression of the form:

$$\exists^{I_1}x_1, ..., \exists^{I_1}x_n : \psi(x_1, ..., x_n)$$

where $I_i = [a_i, b_i]$ are intervals, $\psi(x_1, ..., x_n)$ is a Boolean combination of atomic formulas of the form $g(x_1, ..., x_n)\ \mathtt{op}\ 0$, where g is a composition of Type 2-computable functions and $\mathtt{op} \in \{<, \le, >, \ge, =, \ne\}$.

Note that any bounded Σ_1 sentence is equivalent to a Σ_1 sentence in which all the atoms are of the form $f(x_1, ..., x_n) = 0$ (*i.e.*, the only $\mathtt{op}$ needed is '='). Essentially, Type 2-computable functions can be approximated arbitrarily well by finite computations of a special kind of Turing machines (Type 2 machines); most 'useful' functions over the reals are Type 2-computable. The notion of δ-weakening of a bounded sentence is central to δ-satisfiability.

Definition 3 Let $\delta \in \mathbb{Q}^+ \cup \{0\}$ be a constant and ϕ a bounded Σ_1-sentence in the standard form

$$\phi = \exists^{I_1} x_1, ..., \exists^{I_n} x_n : \bigwedge_{i=1}^{m} (\bigvee_{j=1}^{k_i} f_{ij}(x_1, ..., x_n) = 0) \quad (1)$$

where $f_{ij}(x_1, ..., x_n) = 0$ are atomic formulas. The δ-*weakening* of ϕ is the formula:

$$\phi^\delta = \exists^{I_1} x_1, ..., \exists^{I_n} x_n : \bigwedge_{i=1}^{m} (\bigvee_{j=1}^{k_i} |f_{ij}(x_1, ..., x_n)| \leq \delta) \quad (2)$$

Note that ϕ implies ϕ^δ, while the converse is obviously not true. The bounded δ-satisfiability problem asks for the following: given a sentence of the form (1) and $\delta \in \mathbb{Q}^+$, correctly decide whether **unsat** (ϕ is false), or **δ-sat** (ϕ^δ is true). If the two cases overlap either decision can be returned: such a scenario reveals that the formula is *fragile* - a small perturbation (*i.e.*, a small δ) can change the formula's truth value.

A qualitative property of hybrid systems that can be checked is bounded δ-reachability. It asks whether the system reaches the unsafe region after $k \in \mathbb{N}$ discrete transitions.

Definition 4 Bounded k step δ-reachability in hybrid systems can be encoded as a bounded Σ_1-sentence

$$\begin{aligned} &\exists \mathbf{x}^0_{0,q_0}, \exists \mathbf{x}^t_{0,q_0}, ..., \exists \mathbf{x}^0_{0,q_m}, \exists \mathbf{x}^t_{0,q_m}, ..., \exists \mathbf{x}^0_{k,q_m}, \exists \mathbf{x}^t_{k,q_m} : \\ &\qquad (\bigvee_{q \in Q} (\text{init}_q(\mathbf{x}^0_{0,q}) \wedge \text{flow}_q(\mathbf{x}^0_{0,q}, \mathbf{x}^t_{0,q}))) \\ &\qquad \wedge (\bigwedge_{i=0}^{k-1} (\bigvee_{q,q' \in Q} (\text{jump}_{q \to q'}(\mathbf{x}^t_{i,q}, \mathbf{x}^0_{i+1,q'}) \\ &\wedge (\text{flow}_{q'}(\mathbf{x}^0_{i+1,q'}, \mathbf{x}^t_{i+1,q'}))) \wedge (\bigvee_{q \in Q} \text{unsafe}_q(\mathbf{x}^t_{k,q})))) \end{aligned} \quad (3)$$

where $\mathbf{x}^0_{i,q}$ and $\mathbf{x}_{i,q}$ represent the continuous state in the mode q at the depth i, and q' is a successor mode.

Intuitively, the formula above can be understood as follows: the first conjunction is asking for a set of continuous variables which satisfy the initial condition in one of the modes and the flow in that mode; the second conjunction is looking for a set of vectors which satisfy any k discrete jumps and flows in each successor mode defined by the jumps; the third conjunction is verifying whether the state of the system (the mode and the set of continuous variables in the mode after k jumps) belongs to the unsafe region. Note that the previous definition asks for reachability in *exactly* k steps. One can build a disjunction of formula (3) for all values from 1 to k, thereby obtaining reachability *within* k steps.

The δ-reachability problem can be solved using the described δ-complete decision procedure, which will correctly return one of the following answers:
- **unsat**: the system never reaches the bad region U,
- **δ-sat**: the δ-perturbation of (3) is true, and a witness, *i.e.*, an assignment for all the variables, is returned.

We now show that this δ-decisions technique for hybrid models can be used to handle problems such as model falsification, parameter estimation, and parametric sensitivity analysis.

Model Falsification. The model falsification problem with existing experimental observations is basically a bounded reachability question: Expressing each experimental observation as a goal region, is there any number of steps k in which the model reaches the goal region? If none exists, the model is incorrect regarding the given observation. If, for each observation, a witness is returned, we can conclude that the model is correct with regard to a given set of experimental results. This is a bounded Model Checking problem, where all experimental observations can be expressed as reachability properties.

Parameter Estimation. The parameter estimation problem can also be encoded as a k-step reachability problem: Does it exist a parameter combination for which the model reaches the given goal region in k steps? Considering an assignment of a certain set of system parameters, if a witness is returned, this assignment is potentially a good estimation for those parameters. The goal here is to find an assignment with which all the given goal regions can be reached in bounded steps.

Parametric Sensitivity Analysis. The sensitivity analysis can be conducted by a set of bounded reachability queries as well. For different possible values of a certain system parameter, are the results of reachability analysis the same? If so, the model is insensitive to this parameter with regard to the given experi-mental observations.

4. FORMAL ANALYSIS RESULTS

4.1 Effect of delay in turning light ON

First, we have studied the relation between the time to turn ON the light after adding IPTG ($t_{lightON}$), and the total time needed until the bacteria cells being killed (t_{total}). We fixed the values of several other parameters as follows.
- SOX_{thres} = 5e-4m - threshold for the concentration level of SOX which is sufficient to kill the bacteria cells
- $t_{lightOFF_1}$ = 2 time units (t.u.) - time to turn the light OFF after turning it ON
- $t_{lightOFF_2}$ = 2 t.u. - time to turn the light OFF after removing IPTG
- t_1 = 1 t.u. - time to inject genome
- t_2 = 1 t.u. - time to insert genome into DNA after injecting it into bacteria cell
- $t_{addIPTG_3}$ = 1 t.u. - time to add IPTG after inserting phage genome into bacteria DNA

As shown in the first two rows of Table 2, the earlier we turn on the light after adding IPTG, the quicker the bacteria cells will be killed.

4.2 Lower bound for the duration of exposure to light

The δ-decisions technique has also been adopted to analyze the impact of the time duration that the cells are exposed to light ($t_{lightOFF_1}$) on the system, and estimate an appropriate range for $t_{lightOFF_1}$ which leads to the successful killing of bacteria cells by KillerRed. By setting SOX_{thres}, $t_{lightOFF_2}$, t_1, t_2, and $t_{addIPTG_3}$ with the same values in Section 4.1, and assigning 2 t.u. to $t_{lightON}$ (time to turn the light OFF after turning it ON), we have found that, in order to kill bacteria cells, the system has to keep the light ON for at least 4 time units (see row 3-4 of Table 2).In addition, we have also found that the bacteria cells can be killed within 100 time units when light is ON for 4 time units.

$t_{lightON}$ (t.u.)	1	2	3	4	5	6	7	8	9	10
t_{total} (t.u.)	16	17.2	18.5	20	21.3	22.7	23.5	24.1	25	30
$t_{lightOFF_1}$ (t.u.)	1	2	3	4	5	6	7	8	9	10
killed bacteria cells	failed	failed	failed	succ	succ	succ	succ	succ	succ	succ
t_{rmIPTG_3} (t.u.)	1	2	3	4	5	6	7	8	9	10
killed bacteria cells	succ	succ	succ	succ	succ	succ	succ	succ	succ	succ
SOX_{thres} (M)	1e-4	2e-4	3e-4	4e-4	5e-4	6e-4	7e-4	8e-4	9e-4	1e-3
t_{total} (t.u.)	5.1	5.2	5.4	17	19	48	61	71	36	42

Table 2: Formal analysis results for our KillerRed hybrid model

4.3 Time to remove IPTG as an insensitive role

The sensitivity of the time difference between removing the light and removing IPTG (t_{rmIPTG_3}) with regard to the successful killing of bacteria cells has also been studied. We have noticed that t_{rmIPTG_3} has insignificant impacts on the cell killing outcome (see row 5-6 of Table 2). This is in accordance with our understanding of this system, since any additional KillerRed that will be synthesized will not be activated in the absence of light. Note that, for other involved system parameters, we used the same values for SOX_{thres}, $t_{lightON}$, $t_{lightOFF_2}$, t_1, t_2, and $t_{addIPTG_3}$ as in Section 4.2, and set $t_{lightOFF_1}$ as 4 t.u..

4.4 Necessary level of superoxide

Finally, we have used the δ-decisions to discuss the correctness of our hybrid model by considering various values of SOX_{thres} within the suggested range - [100uM, 1mM]. We have used the same values for variables SOX_{thres}, $t_{lightON}$, $t_{lightOFF_1}$, $t_{lightOFF_2}$, t_1, t_2, and $t_{addIPTG_3}$ as in Section 4.3. As we can see from row 7-8 of Table 2, the bacteria cells can be killed in reasonable time for all 10 point values of SOX_{thres}, which was uniformly chosen from [100uM, 1mM]. Furthermore, we have also found a broader range for SOX_{thres} - (0M, 0.6667M], with which bacteria cells can be killed by KillerRed.

5. CONCLUSION

In this work, we have studied a novel method of killing bacteria using bacteriophage instead of antibiotics. A bacteriophage can be engineered to include code for proteins, which when inside bacteria can get activated and result in bacteria killing. Specifically, in this work we studied photosensitizing proteins, those that produce reactive oxygen species (ROS) when exposed to light. Excess amounts of ROS result in cell death. We created a hybrid model expressing both continuous and discrete dynamics. We defined this model within each of the stages that bacteria can go through, and used our tool (implemented the δ-decisions technique) for hybrid system reachability analysis to define parameters of the model that are otherwise hard or not possible to be found in experiments. We were especially interested in the timing effects, when the cells should be exposed to light, how long the light exposure should be, and how long it takes photosensitized proteins to kill bacteria cells after exposure to light.

Our analysis shows that the timing will be critical if this treatment, using bacteriophage and photosensitized proteins, is used for killing bacteria: the delay in exposure to light can significantly delay bacteria killing and could potentially lead to complications such as sepsis; and the duration of exposure to light is critical - turning light off too early may also not result in killing. Interestingly, we found that a broader range of SOX could kill bacteria, although the time to reach this effect may again be too long for practical purposes. We noticed that very low levels of SOX are efficient in bacteria killing, while medium levels result in the longest time to killing, and we are further investigating these results, as they point to potential improvements in our model. Our next step is to validate the results that we obtained with wet lab experiments, and to use guidance from the experiments to improve accuracy of the model.

6. REFERENCES

[1] Antibiotic resistance threats in the united states. The Center for Disease Control, 2013.

[2] Carnegie mellon university, igem. `http://2013.igem.org/Team:Carnegie_Mellon`, 2013.

[3] B. Bowen and N. Woodbury. Single-molecule fluorescence lifetime and anisotropy measurements of the red fluorescent protein, dsred, in solution. *Photochemistry and photobiology*, 77(4):362–369, 2003.

[4] M. Falconi, P. O'Neill, M. E. Stroppolo, and A. Desideri. Superoxide dismutase kinetics. *Methods in enzymology*, 349:38–49, 2002.

[5] S. Gao, S. Kong, and E. M. Clarke. dReal: An SMT solver for nonlinear theories over the reals. In *CADE*, pages 208–214. Springer, 2013.

[6] S. Gao, S. Kong, and E. M. Clarke. Satisfiability modulo ODEs. In *FMCAD*, pages 105–112, Oct. 2013.

[7] H. Karadag and R. Bilgin. Purification of copper-zinc superoxide dismutase from human erythrocytes and partial characterization. *Biotechnology & Biotechnological Equipment*, 24(1):1653–1656, 2010.

[8] S. Pletnev, N. G. Gurskaya, N. V. Pletneva, K. A. Lukyanov, D. M. Chudakov, V. I. Martynov, et al. Structural basis for phototoxicity of the genetically encoded photosensitizer killerred. *Journal of Biological Chemistry*, 284(46):32028–32039, 2009.

[9] L. Song, E. Hennink, I. T. Young, and H. J. Tanke. Photobleaching kinetics of fluorescein in quantitative fluorescence microscopy. *Biophysical journal*, 68(6):2588, 1995.

[10] K. Takemoto, T. Matsuda, N. Sakai, D. Fu, M. Noda, S. Uchiyama, I. Kotera, Y. Arai, M. Horiuchi, K. Fukui, et al. Supernova, a monomeric photosensitizing fluorescent protein for chromophore-assisted light inactivation. *Scientific reports*, 3, 2013.

[11] R. Y. Tsien and A. Waggoner. Fluorophores for confocal microscopy: Photophysics and photochemistry. In *Handbook of biological confocal microscopy, 3rd edition*. Springer, 2006.